Effect of solute nature on the polyamorphic transition in glassy polyol aqueous solutions

Yoshiharu Suzuki

Citation: The Journal of Chemical Physics **147**, 064511 (2017); doi: 10.1063/1.4998201
View online: http://dx.doi.org/10.1063/1.4998201
View Table of Contents: http://aip.scitation.org/toc/jcp/147/6
Published by the American Institute of Physics

Effect of solute nature on the polyamorphic transition in glassy polyol aqueous solutions

Yoshiharu Suzuki[a)]
Research Center for Advanced Measurement and Characterization, National Institute for Materials Science (NIMS), Namiki 1-1, Tsukuba, Ibaraki 305-0044, Japan

(Received 11 May 2017; accepted 28 July 2017; published online 14 August 2017)

I examined the polyamorphic behavior of glassy dilute aqueous solutions of polyols (ethylene glycol, glycerol, *meso*-erythritol, xylitol, and D-sorbitol) under pressure at low temperatures. Although the volume change of the glassy aqueous solution varied continuously against pressure, the rate of the volume change appeared to vary discontinuously at the onset pressure of the gradual polyamorphic transition. It is thought that low-density liquid-like solvent water and high-density liquid-like solvent water coexist during the transition. Moreover, the existence of a solute induces the shift of polyamorphic transition to the lower-pressure side. The effect of a solute on the polyamorphic transition becomes larger in the order ethylene glycol, glycerol, *meso*-erythritol, xylitol, and D-sorbitol. Therefore, the solute can become a variable controlling the polyamorphic state of liquid water. This experimental result suggests that the metastable-equilibrium phase boundary between the low-density and the high-density amorphs for pure water is likely to be located at 0.22–0.23 GPa at about 150 K, which is slightly larger than the previously estimated pressure. Moreover, the solute-nature dependence on the polyamorphic transition seems to connect to that on the homogeneous nucleation temperature of polyol aqueous solution at ambient pressure. The region in which a low-density liquid appears coincides with the region in which the nucleus of ice Ih appears, suggesting that the formation of a low-density liquid is a precursory phenomenon of the nucleation of ice Ih. *Published by AIP Publishing.* [http://dx.doi.org/10.1063/1.4998201]

I. INTRODUCTION

Recent studies of the amorphous ices of pure water and supercooled liquid water suggest that two kinds of liquid water, low-density liquid (LDL) and high-density liquid (HDL), exist at low temperatures and a liquid-liquid critical point (LLCP) relating to the two kinds of water exists.[1–3] The computer simulation studies using ST2 and TIP4P/2005 water potential models have proven that the LDL and HDL coexist and that the LLCP exists.[4–9] Therefore, the LLCP hypothesis is not an absurd story. In the experimental studies, it is practically difficult to probe the location of the LLCP directly because of the crystallization.[10] It is thought that the virtual LLCP is experimentally undetectable.[11] On this account, the validity of LLCP hypothesis is still actively discussed. However, the accumulated experimental results for the two glassy waters (low-density amorph, LDA, and high-density amorph, HDA, which are corresponding to LDL and HDL, respectively) and for supercooled liquid water around the LLCP are consistent with the LLCP hypothesis of water.[3,12] The experimental facts[13–16] suggest indirectly that the LLCP hypothesis is valid. Therefore, assuming the validity of the LLCP hypothesis in this paper, I will discuss about the polyamorphic behavior of aqueous solutions.

In the present state, it is inferred that the location of the LLCP for H_2O will be around 221–225 K and 0.02–0.05 GPa.[17,18] And then, the fluctuation between LDL and HDL generated around the LLCP will affect the behavior of liquid water at ambient pressure at room temperature.[19] When high-temperature liquid water at ambient pressure that is categorized in the HDL group is cooled, it continuously transfers to liquid water of the LDL-like state across the Widom line.[14,16] This crossover between the HDL-like state and the LDL-like state may cause the anomalous behavior of low-temperature liquid water, for example, the maximum density of liquid water at 277 K and so on.[1,3]

It is reasonable to conceive that the fluctuation between two states of liquid water around the LLCP affects the behavior of not only pure water but also aqueous solutions under ambient condition. Previously, we have reconsidered the state of solvent water in the glassy dilute lithium chloride (LiCl) aqueous solution[20–22] and the glassy dilute glycerol aqueous solution[12,23] from a viewpoint of the LLCP hypothesis and discussed their polyamorphic behavior such as a polyamorphic transition and a nanosegregation of aqueous solutions. These experimental results prove that the existence of a solute affects the polyamorphic transition of solvent water.[22,23] On the other hand, we have demonstrated that the polyamorphic change of solvent water in the glassy glycerol aqueous solution induces the obvious change of the molecular vibration modes of a glycerol molecule.[12] Kim *et al.* have also reported that the polyamorphic change of solvent water confined in the crystalline protein induces the change of the high-order structure of the protein.[24] These experimental results suggest a possibility that the polyamorphic fluctuation of water relates to the

a)Author to whom correspondence should be addressed: suzuki.yoshiharu@nims.go.jp. Telephone: +81-29-860-4877.

structural stability and dynamics of the solute molecule.[12,24–27] Therefore, it is significant to understand the relationship between the solute molecule and the polyamorphic state of water near the solute molecule. However, there are a few studies tackling the problem of basic relationships between the simple solute molecule and two liquid waters, such as the effect of the existence of a solute on the polyamorphic behavior of pure water, the interactions between the solute and the LDL (or HDL), the structural similarity between interfacial water of the solute and the LDL (or HDL), and so on.[12,22,23,28–38] In particular, there are few "high-pressure" studies of the polyamorphic behavior of aqueous solutions[22,23,28,30,31,33,39–41] even though the difference between two polyamorphic states of solvent water appears more clearly under pressure.

Previously, we have experimentally examined the polyamorphic behavior of solvent water in the glassy dilute glycerol aqueous solution under pressure.[23] We have demonstrated that the stepwise volume change of the glassy aqueous solution occurs reversibly by the change in pressure at low temperatures. The Raman spectroscopic study has shown that the state of solvent water in the high-density glassy sample resembles the state of HDA and the state of solvent water in the low-density glassy sample resembles the state of LDA. This suggests that the stepwise volume change of the dilute glassy glycerol aqueous solution relates closely to the HDA-LDA transition of pure water. This experimental result has been supported by the computer simulation study performed by Jahn *et al.*[38] Moreover, the polyamorphic transition of the glassy glycerol aqueous solution shifted toward the lower-pressure side with the increase in glycerol concentration. A coexistent region of LDL-like and HDL-like solvent waters seemed to appear during the polyamorphic transition. The appearance of the coexistent region is consistent with the recent theoretical studies which suggested that an equilibrium coexistent region appears between the low-density and the high-density states in an aqueous solution.[42,43] A similar appearance of the metastable-equilibrium coexistent region has been observed for the glassy dilute LiCl aqueous solutions,[22] although the size of the metastable-equilibrium coexistent region is considerably different from that for the glassy glycerol aqueous solution. The size and location of the equilibrium coexistent region may depend on the solute nature and the concentration.[42] We conjecture that the appearance of the metastable-equilibrium coexistent region relates to the difference between the solute-LDL interaction and the solute-HDL interaction. However, the interactions between the solute and two waters do not yet clarify.

In this study, in order to reconfirm the previous experimental results of the polyamorphic behavior of glycerol-water solutions[23] and in order to understand the effect of solute nature on the polyamorphic behavior of aqueous solutions, I examined the polyamorphic behavior of the glassy aqueous solution of various polyol substances (ethylene glycol, glycerol, *meso*-erythritol, xylitol, and D-sorbitol) under pressure. These polyol solutes are simple organic molecules with the OH groups and are the suitable solute molecules for studying systematically the effect of molecular size and the effect of the hydrogen bonding interaction between the solute and interfacial water on the polyamorphic behavior of solvent water. Therefore, the basic knowledge acquired from the study on the polyamorphic behavior of the polyol aqueous solution contributes to the development of an understanding of the relation between the solute and solvent water.

II. EXPERIMENTAL METHOD

The high-pressure vitrification method of dilute aqueous solutions and the experimental method for the measurement of polyamorphic transition under pressure in this study are almost the same as those in the previous study for the glycerol aqueous solution.[23]

A. Sample

The polyol substances used as a solute in this study are ethylene glycol (EG), glycerol (GL), *meso*-erythritol (ER), xylitol (XY), and D-sorbitol (SO). The number of OH groups and the number of carbons in the polyol molecule increment in the order EG_2, GL_3, ER_4, XY_5, SO_6, where the subscript stands for the number of OH groups or carbon atoms (see molecular structures in Fig. 1).

The polyol solute was mixed with high-purity H_2O (Millipore: Direct-Q UV). The solute concentration, x, of EG_2, GL_3, ER_4, XY_5, and SO_6 aqueous solutions are in the range of 0.03-0.08, 0.02-0.05, 0.02-0.05, 0.02-0.05, and 0.02-0.05, respectively, where x is the ratio of solute molar number to the sum of solute molar number and water molar number. In order to hinder the crystallization of dilute aqueous solutions, polyol aqueous solutions were emulsified. The emulsion sample was made by high-speed blending 1 g of sample solution and a matrix (0.75 g of methylcyclohexane, 0.75 g of methylcyclopentane, and 10 mg of sorbitan tristearate) for 1 min using a homogenizer (OMNI International: Omni TH) with 30 000 rpm. The emulsion size is 1–10 μm in diameter. In order to compare the present experimental results with the previous result of the GL_3 aqueous solution, the same emulsification procedure was used. The influence of emulsification procedure on the polyamorphic behavior of pure water and aqueous solutions has been reported by Hauptmann *et al.*[44]

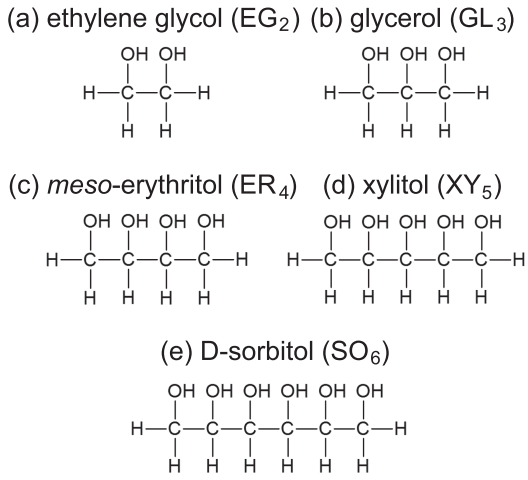

FIG. 1. Structural formula of polyol used in this study. (a) Ethylene glycol (EG_2). (b) Glycerol (GL_3). (c) *Meso*-erythritol (ER_4). (d) Xylitol (XY_5). (e) D-sorbitol (SO_6).

According to their report, the emulsification procedure in this study little influences the freezing and transition of aqueous solutions.

B. Pressure device for high-pressure experiment

A piston-cylinder apparatus and an indium container were used for the high-pressure experiment. The cross section of the piston-cylinder apparatus with the indium container is illustrated in Fig. 2.

The cylinder temperature, T_{cy}, was measured by an alumel-chromel thermocouple attached on the cylinder (thermocouple 1 in Fig. 2) and was controlled by the balance of the attached heater and the atmosphere of cold nitrogen gas.

In order to measure the change in the sample temperature and the relative change in the sample volume simultaneously with the change in pressure, a special indium container with an alumel-chromel thermocouple (thermocouple 2 in Fig. 2) was used.[23] The thermocouple was placed inside the sample. It is experimentally confirmed that the presence of thermocouple hardly influences the polyamorphic behavior of the sample or the crystallization of the sample.

C. Preparation of high-density glassy sample

In general, when the dilute aqueous solution is cooled at 1 atm, a part of solvent water crystallizes to ice Ih and then the segregation to the water-rich crystalline part and the solute-rich glassy part occurs. In order to examine the polyamorphic behavior of dilute aqueous solutions, it is necessary to prepare the homogeneous glassy sample in which the solute molecules disperse homogeneously. Accordingly, I cooled the dilute aqueous solution under high pressure[45,46] and made a homogeneous high-density glassy sample consisting of the HDA-like solvent water as the starting sample.[21–23]

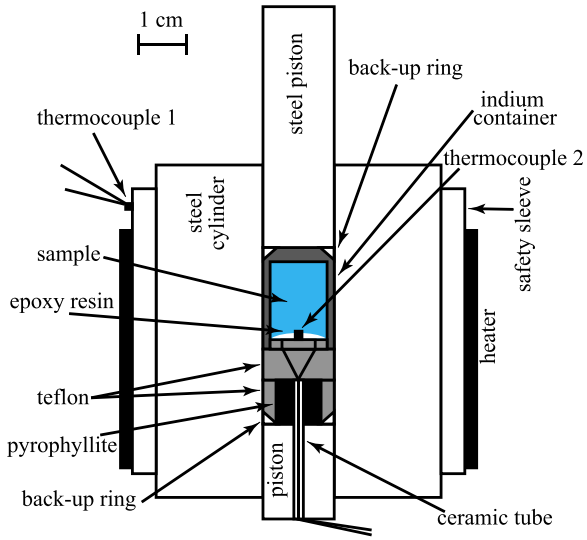

FIG. 2. The cross sections of a piston-cylinder pressure device and of an indium container with a thermocouple for the measurement of sample temperature under pressure. Thermocouples 1 and 2 are for the measurements of the cylinder temperature and of the sample temperature, respectively.

About 1.5 ml of the emulsified sample was sealed in the indium container at 1 atm, compressed to 0.3 GPa at room temperature by using the piston-cylinder apparatus, and then cooled to 77 K at a cooling rate of ~40 K/min as shown in Fig. 3. I measured the change in the sample temperature during the cooling process and verified there was no occurrence of an exothermic event relating to the crystallization of solvent water. Previously, we have checked using Raman spectroscopy that the sample made by the high-pressure cooling process without the exothermic event contains no crystalline parts.[23] In this study, the EG_2 aqueous solution below $x = 0.02$ and the GL_3, ER_4, XY_5, and SO_6 aqueous solutions below $x = 0.01$ crystallized. The check of the crystallization of the sample using the X-ray diffraction method is desirable, but not done in this study.

D. Measurement method of the polyamorphic transition

A typical experimental protocol of this study is shown in Fig. 3. The high-density glassy sample made by cooling at 0.3 GPa was further compressed to 0.6 GPa at 77 K and the piston-cylinder with the sample was heated to a given T_{cy}. The sample is decompressed from 0.6 to 0.01 GPa while maintaining at T_{cy}, kept at 0.01 GPa for 2 min and then compressed to 0.6 GPa at T_{cy}. The decompression/compression rate may affect the experimental results of the polyamorphic behavior such as transition pressure. Therefore, the decompression/compression rate was fixed at ~1.6 MPa/s throughout the measurement. During the decompression and compression processes, the change in the piston displacement, d, and the change in the sample temperature, T_{smp}, were measured simultaneously. The effect of the change in T_{smp} on T_{cy} is little because the amount of sample is remarkably less than that of

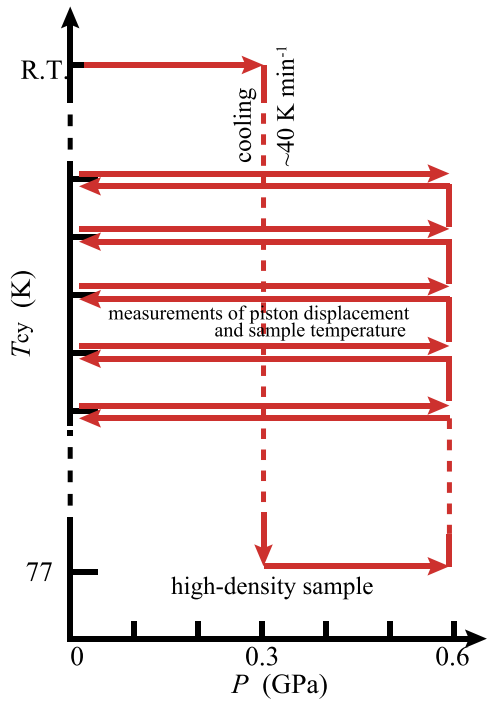

FIG. 3. Temperature-pressure steps for the preparation of the glassy high-density sample and for the measurement of polyamorphic transition.

the piston-cylinder. The change of d corresponds to the relative change of sample volume.

The high-pressure measurement of polyamorphic transition was performed in the T_{cy} range from 130 to 160 K. T_{cy} was increased from the lower temperature and the interval of T_{cy} is ~2 K as shown in Fig. 3. The glassy sample crystallized during or after the polyamorphic transition from high- to low-density state in the decompression process at higher T_{cy}. For example, the glassy EG_2 aqueous solution of $x = 0.03$ crystallized after the polyamorphic transition in the decompression process at T_{cy} = ~148 K. I judged the occurrence of the crystallization from an extremely large increase of T_{smp} because the heat generation caused by the crystallization is larger than that due to polyamorphic transition.[31] T_{cy} at which the crystallization of the glassy sample occurs depends on the solute nature and the solute concentration.

The error of pressure, caused by the friction between the piston and cylinder, was corrected by using the compression and decompression curves of an indium container that were obtained in the same experimental condition. The detailed information relating to the correction of pressure is described in Ref. 23.

E. Measurement of homogeneous nucleation temperature

In order to discuss the relation between the homogeneous nucleation and the polyamorphic transition of polyol aqueous solutions, I measured the homogeneous nucleation temperature, T_H, of the emulsified EG_2, GL_3, ER_4, XY_5, and SO_6 aqueous solutions at 1 atm. About 10 μl of the emulsified polyol aqueous solution was cooled from 300 to 77 K at a cooling rate of ~10 K/s and the change of the sample temperature during cooling was measured using a tiny alumel-chromel thermocouple. As shown in the inset graph of Fig. 4, T_H was determined from the exothermic event due to the crystallization of ice Ih. T_H of the EG_2, GL_3, ER_4, XY_5, and SO_6 aqueous solutions at 1 atm are plotted as the function of x in Fig. 4.

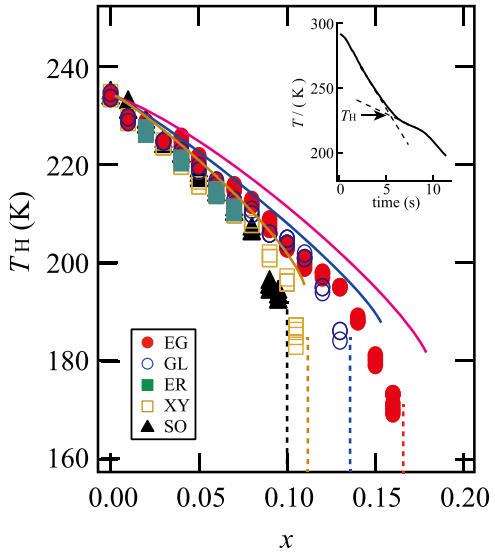

FIG. 4. The homogeneous nucleation temperature, T_H, of polyol aqueous solutions at 1 atm. Filled red circles, open blue circles, filled green squares, open brown squares, and filled black triangles are T_H of the EG_2, GL_3, ER_4, XY_5, and SO_6 aqueous solutions, respectively. As shown in the inset graph, T_H was determined from the exothermic event due to the crystallization. Red, blue, and brown solid curves represent T_H of the EG_2, GL_3, and XY_4 aqueous solutions which are measured by Kanno *et al.* (Ref. 47). The values of x_g for the EG_2, GL_3, XY_5, and SO_6 aqueous solutions are showed by red, blue, brown, and black vertical broken lines, respectively.

In general, T_H depends on the cooling rate. The values of T_H for EG_2, GL_3, and XY_5 aqueous solutions measured in this study are slightly smaller than the results of Kanno *et al.*[47] (Fig. 4) because of the faster cooling rate in this study. T_H becomes lower with the increase in solute concentration, and then when the solute concentration reaches x_g, the aqueous solution does not crystallize and becomes homogeneous glass. x_g as well as T_H depends on the cooling rate. In the case of this study, the values of x_g for the EG_2, GL_3, XY_5, and SO_6 aqueous solutions are ~0.16, ~0.13, ~0.11, and ~0.09, respectively.

The ER_4 aqueous solution of $x > 0.054$ is saturated at room temperature. Therefore, T_H of the ER_4 aqueous solution below $x = 0.05$ is shown in Fig. 4. As the saturated ER_4 aqueous solution still crystallized at low temperatures, x_g of the ER_4 aqueous solution is unidentified in this study.

III. RESULT AND DISCUSSION

A. Determination of polyamorphic transition pressure

The change in d and the change in T_{smp} for the glassy EG_2 aqueous solution of $x = 0.03$ during the decompression and the compression processes at T_{cy} = ~140 K are shown in Fig. 5. Both the polyamorphic transitions from high-density to low-density state and from low-density to high-density state are observed as the exothermic event. This is because the LDA (or HDA) is overdriven into the HDA (or LDA) region as discussed by Whalley *et al.*[48] and by Mishima.[49]

First, I discuss the detailed behavior of the high-density sample during the decompression process [Fig. 5(a)]. In the initial stage from 0.6 to 0.4 GPa [an asterisk part in Fig. 5(a)], the lowering of T_{smp} caused by the quasi-adiabatic volume expansion of the sample was observed. This change of T_{smp} is observed when the rate of decompression (or compression) speed changes and the volume of the sample abruptly changes. Especially, the change of T_{smp} occurs in the initial part of the decompression or compression process. T_{smp} was settled down around 0.4 GPa because of the steady volume change of the sample and the heat balance between the sample and the cylinder. When the pressure is decreased further, a small endothermic event was observed around 0.15 GPa [a point G in Fig. 5(a)] and the slope of the volume change becomes slightly larger at the same time as shown in Fig. 5(b). This indicates that the high-density sample transits from the glassy state to the liquid state. A similar glass-to-liquid transition has been observed for the HDA during isothermal decompression[29] and during isobaric heating[50] and for the high-density glassy aqueous solutions during isothermal decompression[23,31] and during isobaric heating.[41] When the pressure is decreased further, the sample volume increased suddenly around 0.08 GPa and T_{smp} rose a little later. This indicates the polyamorphic transition from the high-density to the low-density sample. We have conjectured recently that the delay of the exothermic

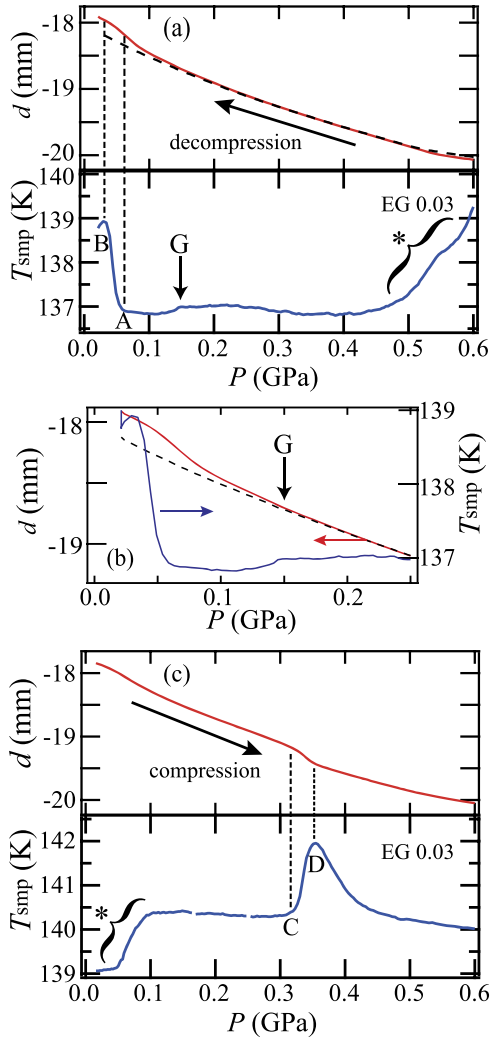

FIG. 5. The change in the piston displacement, d, and the change in the sample temperature, T_{smp}, during (a) the decompression and (c) the compression processes for the EG_2 aqueous solution of $x = 0.03$ at $T_{cy} \sim 140$ K. The change in d and the change in T_{smp}, are shown in the upper and the lower panels, respectively. (a) A black broken curve in the upper panel shows the change in d for the high-density sample at $T_{cy} \sim 130$ K which does not transit to the low-density sample at the lower pressures. Points A and B represent the onset and the offset pressures of the polyamorphic transition from high- to low-density state, respectively. Point G represents a glass-to-liquid transition of high-density sample. (b) The change in d and the change in T_{smp} during the decompression process are expanded in the range of 0.0–0.3 GPa. (c) Points C and D represent the onset and the offset pressures of the polyamorphic transition from low- to high-density state, respectively.

event is caused by the endothermic event due to the sudden increase of sample volume.[23,31] The exothermic event finishes around 0.02 GPa, indicating that the polyamorphic transition is completed.

Next, when the low-density sample is compressed at the same $T_{cy} = \sim 140$ K, the rise of T_{smp} caused by quasi-adiabatic compression is observed in the pressure range from 0.01 to ~0.1 GPa [an asterisk part in Fig. 5(c)]. When the pressure is increased further, the stepwise decrease in the sample volume and the large increase in T_{smp} occur simultaneously around 0.32 GPa. This indicates the polyamorphic transition from the low-density to the high-density sample. The exothermic event finishes around 0.35 GPa and then the polyamorphic transition finishes. The relation between the change in the sample volume and the change in T_{smp} observed during the polyamorphic transition is consistent with the previous experimental result for the glycerol-water system.[23]

In this study, I determined the pressures of the polyamorphic transition, P_{LtoH} and P_{HtoL}, from the conspicuous change of T_{smp} as shown by an A-B region and a C-D region in Fig. 5, where P_{LtoH} and P_{HtoL} are the pressure of polyamorphic transition from the low-density to the high-density state during the compression process and the pressure of polyamorphic transition from the high-density to the low-density state during the decompression process, respectively. The real onset P_{HtoL} is the pressure at which d starts increasing. The onset P_{HtoL} estimated from the change of T_{smp} is smaller than the real onset P_{HtoL}. However, the change of d at the polyamorphic transition is vaguer than the change of T_{smp} and it is difficult to estimate the accurate value of the onset P_{HtoL} from the change of d. Therefore, in this study I adopted the value of the onset P_{HtoL} estimated from the change of T_{smp}.

B. Temperature and solute-concentration dependences on the polyamorphic transition of glassy polyol aqueous solutions

The temperature and the solute-concentration dependences on the polyamorphic transition for the glassy EG_2, GL_3, ER_4, XY_5, and SO_6 aqueous solutions are shown in Figs. 6–10. The changes in T_{smp} during the compression and the decompression processes are represented by red and blue curves, respectively. The filled circles, open circles, filled squares, and open squares stand for onset P_{LtoH}, offset P_{LtoH}, onset P_{HtoL}, and offset P_{HtoL}, respectively.

The peak of heat generation due to the polyamorphic transition becomes smaller with the increase of the solute concentration. Therefore, the estimation of P_{LtoH} for the high concentration sample becomes difficult, for example, the EG_2 sample of $x = 0.08$, the GL_3 sample of $x = 0.05$, the ER_4 sample of $x = 0.05$, the XY_5 sample of $x = 0.05$, and the SO_6 samples of $x = 0.04$. The error of these P_{LtoH} may be large though I carefully identified the value of P_{LtoH} by expanding these T_{smp} peaks. I could not identify the value of P_{LtoH} for the SO_6 samples of $x = 0.05$ because of the too unclear peak of heat generation.

The light-red belt between the onset and the offset P_{LtoH} and the light-blue belt between the onset and the offset P_{HtoL} in Figs. 6–10 indicate the pressure regions in which the LDL-like and the HDL-like solvent water coexist during the polyamorphic transition. There are theoretical studies that the existence of a solute induces the coexistence of the LDL-like and the HDL-like domain.[42,43] In the previous study on glycerol aqueous solutions, we have inferred that LDL-like and HDL-like solvent water may coexist in the pressure regions shown by the light-red and the light-blue belts though the microscopic state of the coexistence is not proven experimentally.[23]

In the polyamorphic transition for each polyol aqueous solution, as the temperature increases, P_{LtoH} decreases, P_{HtoL} increases, and the width of the hysteresis of polyamorphic transition, which is a difference between the onset P_{LtoH} and the onset P_{HtoL}, becomes narrower. Such tendency of the temperature dependence on the polyamorphic transition is

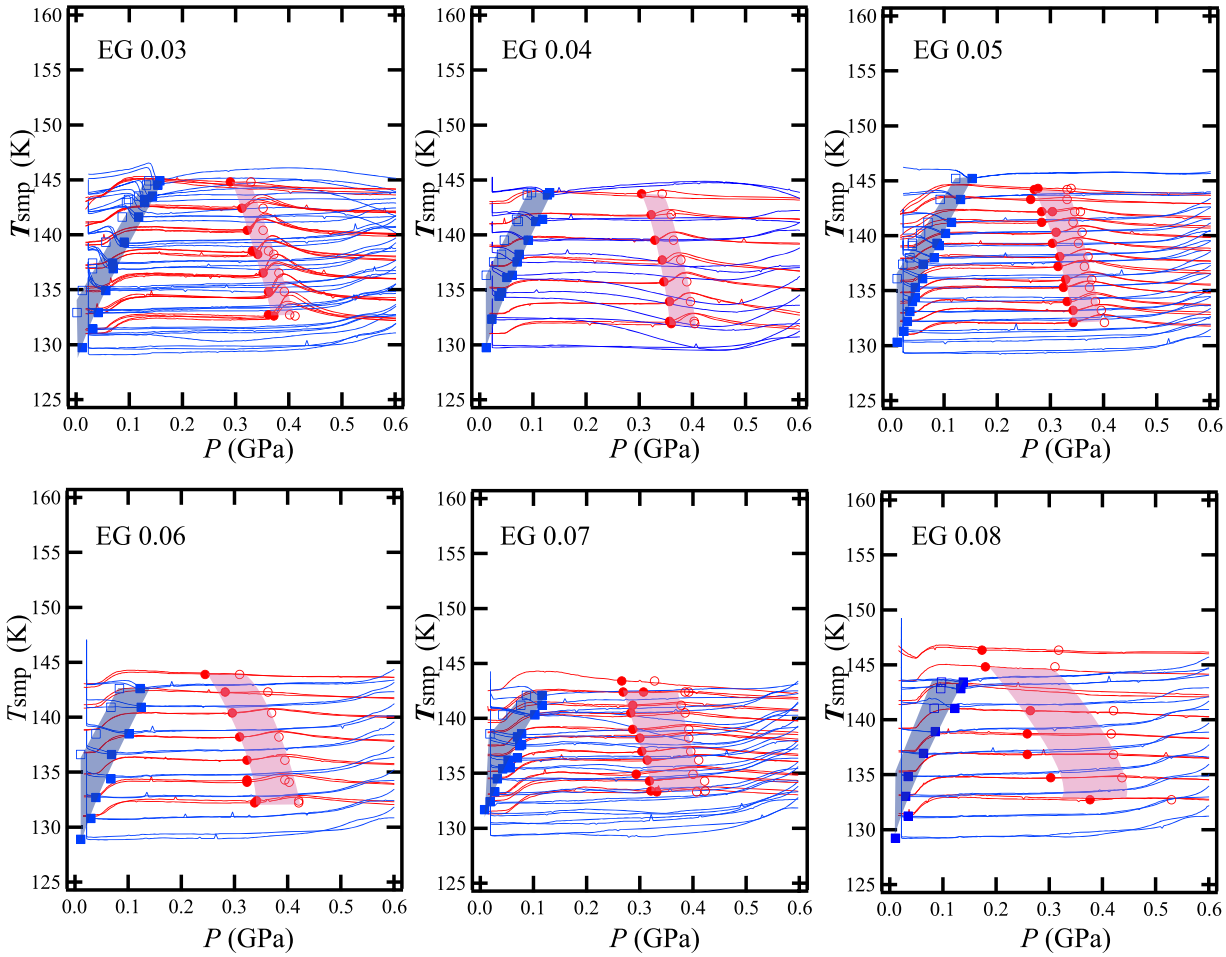

FIG. 6. Temperature dependence on the polyamorphic transition for EG_2 aqueous solutions of $x = 0.03$, 0.04, 0.05, 0.06, 0.07, and 0.08. The changes in T_{smp} during the compression and the decompression processes are drawn by red and blue curves, respectively. The filled circles, open circles, filled squares, and open squares stand for onset P_{LtoH}, offset P_{LtoH}, onset P_{HtoL}, and offset P_{HtoL}, respectively.

analogous to that for the GL_3 aqueous solution in the previous study.[23]

In addition, as the solute concentration increases, the polyamorphic transition shifts toward the lower-pressure side and the width of the light-red belt and the width of the light-blue belt become larger. This tendency of the solute-concentration dependence on the polyamorphic transition is consistent with the previous result for the GL_3 aqueous solution.[23]

I confirmed that the polyamorphic transition of solvent water occurs in the glassy aqueous solution of not only GL_3 but also other polyol solutes. I concluded that the effect of polyol solutes on the polyamorphic behavior is similar.

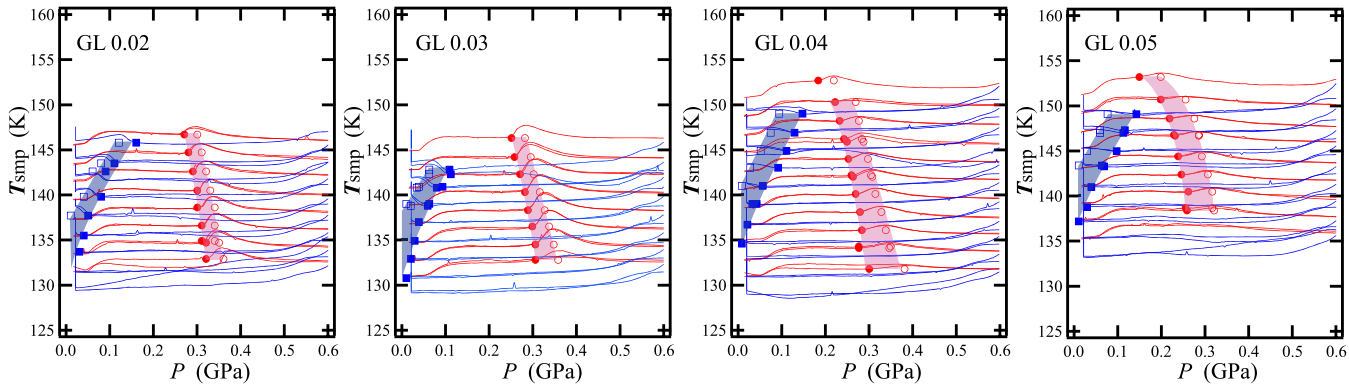

FIG. 7. Temperature dependence on the polyamorphic transition for GL_3 aqueous solutions of $x = 0.02$, 0.03, 0.04, and 0.05. The changes in T_{smp} during the compression and the decompression processes are drawn by red and blue curves, respectively. The filled circles, open circles, filled squares, and open squares stand for onset P_{LtoH}, offset P_{LtoH}, onset P_{HtoL}, and offset P_{HtoL}, respectively.

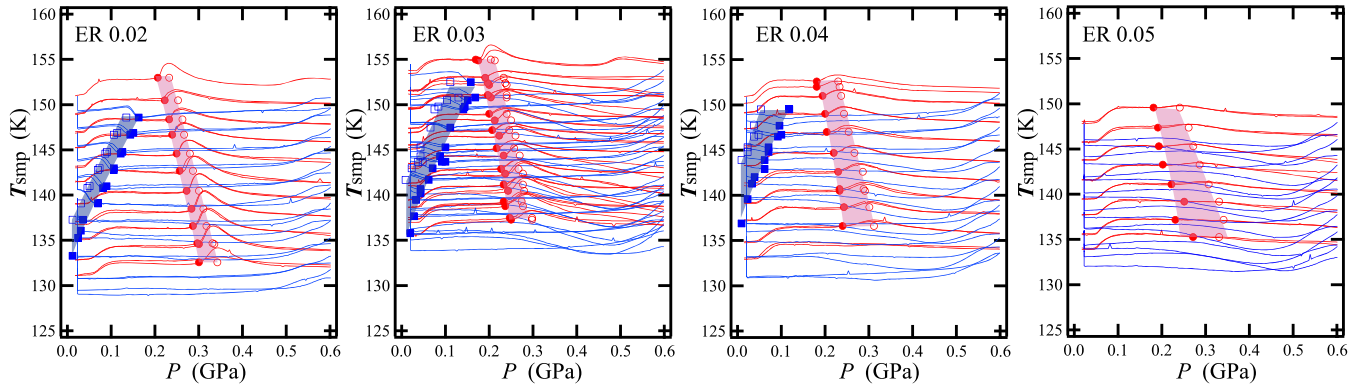

FIG. 8. Temperature dependence on the polyamorphic transition for ER_4 aqueous solutions of $x = 0.02$, 0.03, 0.04, and 0.05. The changes in T_{smp} during the compression and the decompression processes are drawn by red and blue curves, respectively. The filled circles, open circles, filled squares, and open squares stand for onset P_{LtoH}, offset P_{LtoH}, onset P_{HtoL}, and offset P_{HtoL}, respectively.

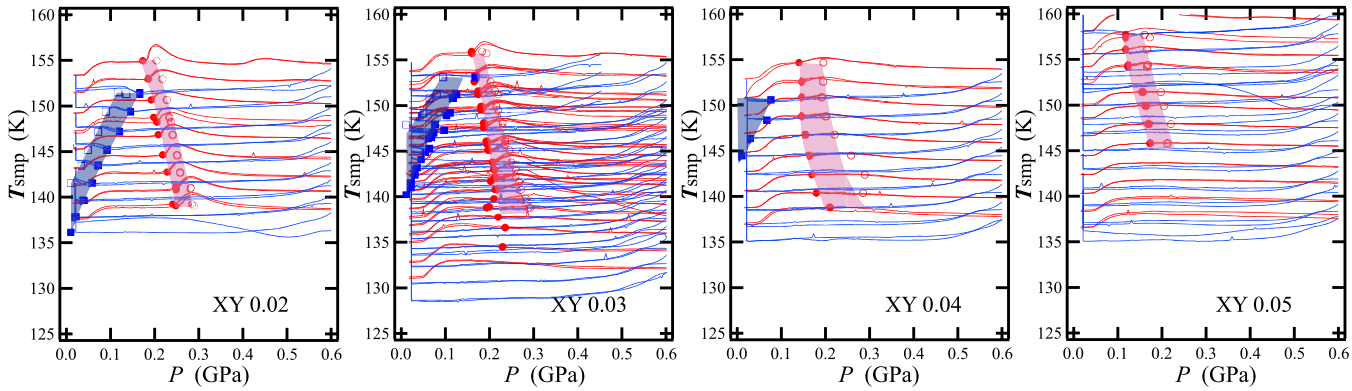

FIG. 9. Temperature dependence on the polyamorphic transition for XY_5 aqueous solutions of $x = 0.02$, 0.03, 0.04, and 0.05. The changes in T_{smp} during the compression and the decompression processes are drawn by red and blue curves, respectively. The filled circles, open circles, filled squares, and open squares stand for onset P_{LtoH}, offset P_{LtoH}, onset P_{HtoL}, and offset P_{HtoL}, respectively.

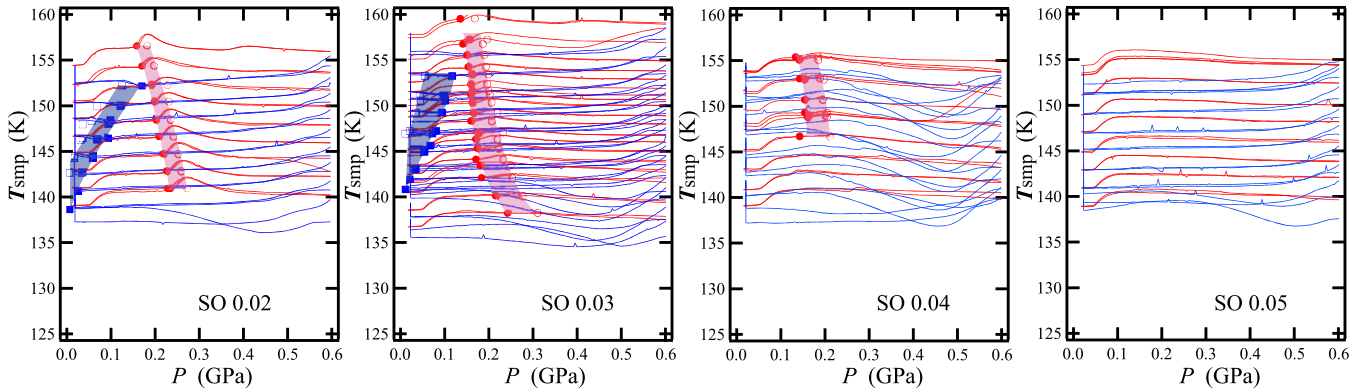

FIG. 10. Temperature dependence on the polyamorphic transition for SO_6 aqueous solutions of $x = 0.02$, 0.03, 0.04, and 0.05. The changes in T_{smp} during the compression and the decompression processes are drawn by red and blue curves, respectively. The filled circles, open circles, filled squares, and open squares stand for onset P_{LtoH}, offset P_{LtoH}, onset P_{HtoL}, and offset P_{HtoL}, respectively.

C. The solute-nature dependence on the polyamorphic transition of glassy polyol aqueous solutions

In order to examine the solute-nature dependence on the polyamorphic behavior, I compare the polyamorphic transitions for each glassy aqueous solution of $x = 0.03$ in Fig. 11. It is found that the polyamorphic transition shifts toward the lower-pressure side in the order EG_2, GL_3, ER_4, XY_5, and SO_6.

In order to discuss the effect of solute nature on the polyamorphic transition more quantitatively, I introduce a new parameter, P_{ecr}, which characterizes the location of the equilibrium coexistent region of the low-density and the high-density states. The equilibrium coexistent region

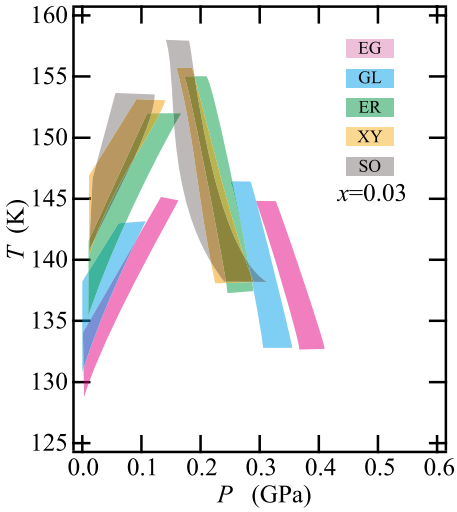

FIG. 11. Dependence of solute nature on the polyamorphic transition for glassy polyol aqueous solutions of $x = 0.03$.

corresponds to a coexistent line of the LDA and HDA for pure water. I suppose that the equilibrium coexistent region will lie somewhere between P_{LtoH} and P_{HtoL} because the polyamorphic transition in this study occurs under a non-equilibrium condition.

Here, I defined P_{ecr} as the middle point between P_{LtoH} and P_{HtoL}, as shown in Fig. 12. The P_{ecr} line in the range between 135 and 145 K is almost vertical to the pressure axis. This is consistent with the suggestion that the liquid-liquid transition (LLT) line for pure water below ~160 K is almost vertical to the pressure axis.[2] P_{ecr} averaged in the range of 135 and 145 K, $\langle P_{\mathrm{ecr}} \rangle$, was plotted as the function of the solute concentration in Fig. 13(a).

$\langle P_{\mathrm{ecr}} \rangle$ for each glassy polyol aqueous solution shifts toward the lower-pressure side with the increase in solute concentration and $\langle P_{\mathrm{ecr}} \rangle$ for each glassy polyol aqueous solution with the same solute concentration becomes smaller in the

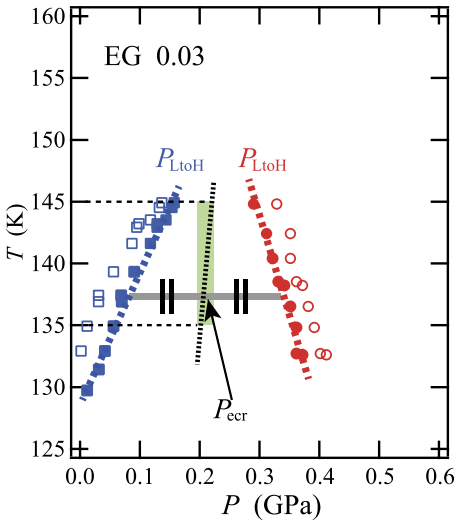

FIG. 12. Description for the definition of P_{ecr}. P_{ecr} is the middle point between onset P_{LtoH} and onset P_{HtoL}. A black dotted line stands for the middle line between the onset P_{LtoH} line and onset P_{HtoL} line. P_{ecr} is averaged in the range of 135 and 145 K (a green band).

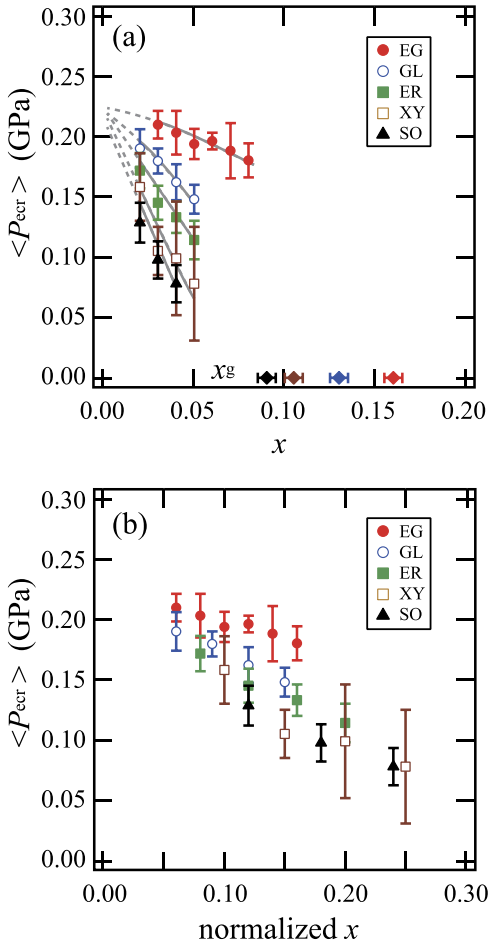

FIG. 13. Solute-concentration dependences on $\langle P_{\mathrm{ecr}} \rangle$ of glassy polyol aqueous solutions. Filled circles (red), open circles (blue), filled squares (green), open squares (brown), and filled triangles (black) are $\langle P_{\mathrm{ecr}} \rangle$ of EG_2, GL_3, ER_4, XY_5, and SO_6 aqueous solutions, respectively. (a) x_g of EG_2, GL_3, XY_5, and SO_6 aqueous solutions (diamonds) are plotted on the concentration axis at ambient pressure. Gray lines are drawn as a guide to the eye. (b) $\langle P_{\mathrm{ecr}} \rangle$ are plotted against the solute concentration normalized by the number of the OH groups or the number of carbons.

order EG_2, GL_3, ER_4, XY_5, and SO_6. This indicates that the effect of the solute on the polyamorphic behavior of solvent water becomes larger in the order EG_2, GL_3, ER_4, XY_5, and SO_6. Moreover, the value of $\langle P_{\mathrm{ecr}} \rangle$ extrapolated to $x = 0$ is 0.22–0.23 GPa and is slightly larger than the pressure of the LDA-HDA transition for pure water below 160 K proposed by Mishima,[2] that is, ~0.20 GPa.

Next, in order to discuss the effect of the number of OH groups (or CH part) in a solute molecule on the polyamorphic transition, $\langle P_{\mathrm{ecr}} \rangle$ is plotted as the function of the concentration normalized by the number of OH groups (or CH part) in Fig. 13(b). The normalized x corresponds to the concentration of the OH group (or CH part) of the aqueous solution. The dependence of the solute nature on $\langle P_{\mathrm{ecr}} \rangle$ shown in Fig. 13(b) becomes smaller than the result shown in Fig. 13(a). This suggests that the presence of the OH group (or CH part) influences the shift of the polyamorphic transition of solvent water. On the other hand, $\langle P_{\mathrm{ecr}} \rangle$ in Fig. 13(b) seems to depend slightly on the solute nature in the order EG_2, GL_3, ER_4, XY_5, and SO_6. Probably, the structure of polyol molecules, for example, the molecular size, the topological symmetry of molecules,

the molecular flexibility, the geometry of OH groups, and so on, may affect the polyamorphic transition of solvent water. However, it is not clear which factor of the solute contributes effectively to the polyamorphic behavior of polyol aqueous solutions. It is necessary to clarify this issue in future. In particular, I think that it is important to study the effects of the presence of the OH group in the solute on the polyamorphic behavior of solvent water because the OH groups of the solute strongly affect the formation of the hydrogen-bonding network of water.

This result that the polyamorphic behavior of solvent water depends on the polyol nature implies that the polyamorphic state of water can be artificially controlled by changing the solute nature and the solute concentration. In other words, the solute as well as pressure, temperature, and confinement can become an external field inducing the polyamorphic change of water.

D. Relation between the nucleation of ice Ih and $\langle P_{ecr} \rangle$

In this section, I will discuss about a relation between the nucleation of crystalline ice Ih in the polyol aqueous solution and the polyamorphic transition of the glassy polyol aqueous solution. As shown in Fig. 4, x_g of the polyol aqueous solutions at 1 atm become smaller in the order EG_2, GL_3, XY_5, and SO_6. This order of x_g coincides with the magnitude relation of $\langle P_{ecr} \rangle$ for the glassy EG_2, GL_3, XY_5, and SO_6 aqueous solutions of the same solute concentration. As shown in Fig. 13(a), when the $\langle P_{ecr} \rangle$ curve extrapolates to 1 atm, the intersection of each $\langle P_{ecr} \rangle$ curve and the x axis seems to be located near the corresponding x_g. This suggests that the nucleation of ice Ih and the polyamorphic behavior of solvent water in the aqueous solution are closely connected with each other.

Assuming that the curvature of the metastable-equilibrium coexistent region on the P-x plane is similar to the curvature of the $\langle P_{ecr} \rangle$ curve, the metastable-equilibrium coexistent regions of polyol aqueous solutions may be schematically drawn such as the colored regions in Fig. 14. However, it is difficult to draw the correct figure of the metastable-equilibrium coexistent region from the experimental information in this study.

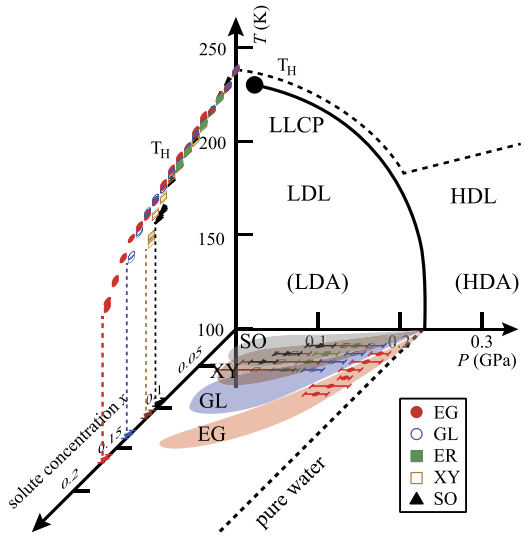

FIG. 14. A schematic polyamorphic P-T-x phase diagram of polyol aqueous solutions. The coexistent regions drawn on the P-x plane are speculation.

The relationship between the equilibrium coexistent region in the aqueous solutions and the corresponding T_H curve indicates that the region in which LDL-like solvent water appears agrees with the region in which the nucleation of ice Ih occurs. This suggests that the nucleus of ice Ih is directly created from the LDL and not from the HDL. In other words, the formation of the LDL may be a precursor phenomenon of the nucleation of ice Ih. This suggestion is consistent with the results of the MD simulation studies relating to the crystallization of Ih that the nucleus of ice Ih appears in the LDL region.[8,36,51,52]

In the past experimental studies, there were some discussions about the relation between the polyamorphic transition and the homogeneous nucleation of ice Ih.[23,30] It is thought that the LLT curve of pure water in the P-T plane is parallel to the T_H curve of pure water and rather the two curves almost overlap.[2,30] Similarly, the curvature of the metastable-equilibrium coexistent region of LDL-like and HDL-like solvent water in the glassy LiCl aqueous solution is roughly parallel to the curvature of the T_H curve of the LiCl aqueous solution at 1 atm.[22,30,31] We have suggested that the LLCP of the glassy GL_3 aqueous solution at 150 K is located around x = 0.12 around ~50 MPa and its Widom line runs near x_g of the GL_3 aqueous solution at 1 atm.[23] Moreover, we have inferred that the change in the LLCP of the GL_3 aqueous solution with the change in the solute concentration seems to run parallel to the T_H curve of the GL_3 aqueous solution at 1 atm.[23] These experimental findings suggest that the polyamorphic fluctuation between two liquid waters affects the homogeneous nucleation of ice Ih and support the present conclusion strongly.

IV. CONCLUSION

I examined the polyamorphic transition of solvent water in the glassy dilute aqueous solution of various polyol solutes (EG_2, GL_3, ER_4, XY_5, and SO_6) under pressure and discussed the temperature, the solute-concentration, and the solute-nature dependences on the polyamorphic transition. I confirmed that solvent water in the polyol aqueous solutions underwent the polyamorphic transition relating to the water polyamorphism. As the solute concentration increases, the polyamorphic transition shifts toward the lower-pressure side. Moreover, it is found that the shift of the polyamorphic transition becomes larger in the order EG_2, GL_3, ER_4, XY_5, and SO_6. This indicates that the polyamorphic state of water is able to be controlled by varying the solute concentration and the solute nature. This suggests that the dynamic fluctuation of solute concentration induces the dynamic fluctuation between the LDL-like and the HDL-like state of solvent water. In particular, the polyamorphic fluctuation of solvent water may play the important roles for the self-aggregation of macromolecules, such as a coil-globule transition of a polymer and a folding/unfolding of a protein, because the local density in a single macromolecule fluctuates during the transformation process.

I demonstrated that the solute-nature dependence on the polyamorphic transition of the glassy polyol aqueous solution relates closely to that on T_H of the polyol aqueous solution at 1 atm, indicating that the region of LDL-like solvent water accords roughly with the region in which the nucleation of ice Ih occurs. This suggests that the nucleation of ice Ih occurs via the LDL-like state. The kinetic nucleation of ice Ih may connect closely to the thermodynamic fluctuation between the LDL and HDL derived from the LLCP and LLT. This speculation suggests that the well-known phenomena of low-temperature aqueous solutions, for example, the freezing point depression, the glass forming, the segregation, and so on, relate to the polyamorphic fluctuation of solvent water.

ACKNOWLEDGMENTS

I am grateful to Osamu Mishima for precious discussion and careful review.

[1] P. G. Debenedetti, J. Phys.: Condens. Matter **15**, R1669 (2003).
[2] O. Mishima and H. E. Stanley, Nature **396**, 329 (1998).
[3] P. Gallo, K. Amann-Winkel, C. A. Angell, M. A. Anisimov, F. Caupin, C. Chakravarty, E. Lascaris, T. Loerting, A. Z. Panagiotopoulos, J. Russo, J. A. Sellberg, H. E. Stanley, H. Tanaka, C. Vega, L. Xu, and L. G. M. Pettersson, Chem. Rev. **116**, 7463 (2016).
[4] P. H. Poole, F. Sciortino, U. Essmann, and H. E. Stanley, Nature **360**, 324 (1992).
[5] J. C. Palmer, F. Martelli, Y. Liu, R. Car, A. Z. Panagiotopoulos, and P. G. Debenedetti, Nature **510**, 385 (2014).
[6] R. S. Singh, J. W. Biddle, P. G. Debenedetti, and M. A. Anisimov, J. Chem. Phys. **144**, 144504 (2016).
[7] J. L. F. Abascal and C. Vega, J. Chem. Phys. **133**, 234502 (2010).
[8] T. Yagasaki, M. Matsumoto, and H. Tanaka, Phys. Rev. E **89**, 020301(R) (2014).
[9] T. Sumi and H. Sekino, RSC Adv. **3**, 12743 (2013).
[10] K. Binder, Proc. Natl. Acad. Sci. U. S. A. **111**, 9374 (2014).
[11] V. Holten and M. A. Anisimov, Sci. Rep. **2**, 713 (2012).
[12] Y. Suzuki and O. Mishima, J. Chem. Phys. **145**, 024501 (2016).
[13] O. Mishima and H. E. Stanley, Nature **392**, 164 (1998).
[14] O. Mishima, Phys. Rev. Lett. **85**, 334 (2000).
[15] K. Amann-Winkel, C. Gainaru, P. H. Handle, M. Seidl, H. Nelson, R. Bohmer, and T. Loerting, Proc. Natl. Acad. Sci. U. S. A. **110**, 17720 (2013).
[16] J. A. Sellberg, C. Huang, T. A. McQueen, N. D. Loh, H. Laksmono, D. Schlesinger, R. G. Sierra, D. Nordlund, C. Y. Hampton, D. Starodub, D. P. DePonte, M. Beye, C. Chen, A. V. Martin, A. Barty, K. T. Wikfeldt, T. M. Weiss, C. Caronna, J. Feldkamp, L. B. Skinner, M. M. Seibert, M. Messerschmidt, G. J. Williams, S. Boutet, L. G. M. Pettersson, M. J. Bogan, and A. Nilsson, Nature **510**, 381 (2014).
[17] O. Mishima, J. Chem. Phys. **133**, 144503 (2010).
[18] V. Holten, C. E. Bertrand, M. A. Anisimov, and J. V. Sengers, J. Chem. Phys. **136**, 094507 (2012).
[19] L. Xu, P. Kumar, S. V. Buldyrev, S.-H. Chen, P. H. Poole, F. Sciortino, and H. E. Stanley, Proc. Natl. Acad. Sci. U. S. A. **102**, 16558 (2005).
[20] Y. Suzuki and O. Mishima, Phys. Rev. Lett. **85**, 1322 (2000).
[21] Y. Suzuki and O. Mishima, J. Chem. Phys. **117**, 1673 (2002).
[22] Y. Suzuki and O. Mishima, J. Chem. Phys. **138**, 084507 (2013).
[23] Y. Suzuki and O. Mishima, J. Chem. Phys. **141**, 094505 (2014).
[24] C. U. Kim, M. W. Tate, and S. M. Gruner, Proc. Natl. Acad. Sci. U. S. A. **108**, 20897 (2011).
[25] S.-H. Chen, L. Liu, E. Fratini, P. Baglioni, A. Faraone, and E. Mamontov, Proc. Natl. Acad. Sci. U. S. A. **103**, 9012 (2006).
[26] F. Mallamace, C. Corsaro, P. Baglioni, E. Fratini, and S.-H. Chen, J. Phys.: Condens. Matter **24**, 064103 (2012).
[27] F. Mallamace, P. Baglioni, C. Corsaro, S.-H. Chen, D. Mallamace, C. Vasi, and H. E. Stanley, J. Chem. Phys. **141**, 165104 (2014).
[28] Y. Yoshimura and H. Kanno, J. Phys.: Condens. Matter **14**, 10671 (2002).
[29] O. Mishima, J. Chem. Phys. **121**, 3161 (2004).
[30] O. Mishima, J. Chem. Phys. **123**, 154506 (2005).
[31] O. Mishima, J. Chem. Phys. **126**, 244507 (2007).
[32] Y. Suzuki, Phys. Rev. B **70**, 172108 (2004).
[33] G. N. Ruiz, L. E. Bove, H. R. Corti, and T. Loerting, Phys. Chem. Chem. Phys. **16**, 18553 (2014).
[34] F. Mallamace, C. Corsaro, D. Mallamace, C. Vasi, S. Vasi, and H. E. Stanley, J. Chem. Phys. **144**, 064506 (2016).
[35] L. Le and V. Molinero, J. Phys. Chem. A **115**, 5900 (2011).
[36] G. Bullock and V. Molinero, Faraday Discuss. **167**, 371 (2013).
[37] D. Corradini, M. Rovere, and P. Gallo, J. Phys. Chem. B **115**, 1461 (2011).
[38] D. A. Jahn, J. Wong, J. Bachler, T. Loerting, and N. Giovambattista, Phys. Chem. Chem. Phys. **18**, 11042 (2016).
[39] J. Bachler, V. Fuentes-Landete, D. A. Jahn, J. Wong, N. Giovambattista, and T. Loerting, Phys. Chem. Chem. Phys. **18**, 11058 (2016).
[40] I. Popov, A. Greenbaum (Gutina), A. P. Sokolov, and Y. Feldman, Phys. Chem. Chem. Phys. **17**, 18063 (2015).
[41] O. Andersson and A. Inaba, J. Phys. Chem. Lett. **3**, 1951 (2012).
[42] J. W. Biddle, V. Holten, and M. A. Anisimov, J. Chem. Phys. **141**, 074504 (2014).
[43] S. Chatterjee and P. G. Debenedetti, J. Chem. Phys. **124**, 154503 (2006).
[44] A. Hauptmann, K. F. Handle, P. Baloh, H. Grothe, and T. Loerting, J. Chem. Phys. **145**, 211923 (2016).
[45] O. Mishima and Y. Suzuki, J. Chem. Phys. **115**, 4199 (2001).
[46] C. U. Kim, Y.-F. Chen, M. W. Tate, and S. M. Gruner, J. Appl. Crystallogr. **41**, 1 (2008).
[47] H. Kanno, K. Miyata, K. Tomizawa, and H. Tanaka, J. Phys. Chem. A **108**, 6079 (2004).
[48] E. Whalley, D. D. Klug, and Y. P. Handa, Nature **342**, 782 (1989).
[49] O. Mishima, J. Chem. Phys. **100**, 5910 (1994).
[50] M. Seidl, M. S. Elsaesser, K. Winkel, G. Zifferer, E. Mayer, and T. Loerting, Phys. Rev. B **83**, 100201(R) (2011).
[51] E. B. Moore and V. Molinero, Nature **479**, 506 (2011).
[52] R. S. Singh and B. Bagchi, J. Chem. Phys. **140**, 164503 (2014).